Interactive comment on "Spatiotemporal transformation of dissolved organic matter along an alpine stream flowpath on the Qinghai-Tibetan Plateau: importance of source and permafrost degradation" by Yinghui Wang et al.

R. Jaffe (Referee)
jaffer@fiu.edu
Received and published: 6 June 2018

On behalf of coauthors, I really appreciate Dr. Jaffe to acknowledge the merit of our work and gave many valuable comments. We accepted most of his comments and made corrections in the revised manuscript. The follows are our responses point by point. I also marked all changes in the revised manuscript.

General Comments:
The abovementioned manuscript describes research on the effect of climate change on permafrost degradation in the Tibetan Plateau and its potential impact on associated fluvial systems, in particular on the dynamics of dissolved organic matter. This research is of global significance as little is known about permafrost degradation in areas other than the arctic, and nearly 70% of alpine permafrost is located in the geographical area of this study. The research team is composed of highly qualified scientists with ample experience and expertise in the specific field of study, and applying ideal methodologies to reach the outlines objectives of this research initiative. The manuscript is well written, and the data properly presented. The literature is also properly reviewed and well represented. As such, this manuscript is well-suited for the journal Biogeosciences and I recommend it to be published. However, some aspects of the manuscript should be improved prior to acceptance. For example, seasonal variability observed needs to be fully explained; explanations regarding the observed differences in DOM leachate composition between the AL vs PL needs to be better explained; discussion on instream generation of DOM through microbial primary productivity should be enhanced and variations along the sampling transect better described; etc. These pending issues are described in more detail below.

Specific Comments:
1) L43: ": in-stream metabolism:": Throughout the manuscript make sure DOM degradation via molecular transformations vs mineralization to CO2 is specified as needed. Similarly, dilution (concentration decrease) vs. 'dilution' (change in relative abundance) through mixing with in-stream DOM from microbial PP?
Response: This is a good comment. Since the DOM degradation process is very complex. Besides different types of degradation (photodegradation vs. biodegradation), DOM can be also completely degraded into CO2 or partially degraded to other compounds. For the former, we prefer to call "transformation", while for the latter, we used "mineralization", although in many literatures, "degradation" was simply used for expressing DOM change. In the revised manuscript, we clarify this difference. From

line 41-43, we rewrote as “Our study thus demonstrates that hydrological conditions impact the mobilization of permafrost carbon in an alpine fluvial network, the signature of which is quickly lost through in-stream mineralization and transformation”. As for the dilution effect, we referred it to concentration decease at Line 292-304.

2) L 54: As in #1 – bio- and photo-transformation vs. mineralization? Both?
Response: As we mentioned above, we clarify this point in the revised manuscript. We rewrote the sentence as “When permafrost-derived carbon enters aquatic system, it can be rapidly mineralized and transformed by microbes and light” in line 55.

3) L61-62: Not sure ‘hydrologic inputs’ is the best way to word this! Please re-phrase.
Response: We use ‘hydrologic condition’ to replace ‘hydrologic inputs’.

4) L116: Please indicate distance in Km. This can be deduced from Fig. 1, but would be helpful here for the reader to easily gain a grasp of the spatial extension of the study.
Response: That’s a good suggestion. we suppled this information in the revised manuscript. In line 117-118, we wrote as ‘The water in the gully flows southward across the hillslope before draining into Qinghai Lake, and the total length of the stream is around 40 km (Fig. 1).’

5) L120-124: Please add more details on the methodology used for leachate collection.
Response: We already added the more detailed description of the sampling method in the revised manuscript (Line 122-125). We wrote as ‘At each sampling time, both AL and PL leachates were collected at the depth of 60 cm and 220 cm, respectively, of the gullies’ head. 20 L HDPE carboys were cleaned by pure water, 0.1 N hydrochloric acid and pure water prior to use. It usually took 2 days to gather > 15 L leaching waters. After that, the leachate samples were immediately kept on ice and in the dark by aluminum foil. They were transported to the temporary laboratory in the Gangcha County with six hours.’

6) L124-127+: Please add distances in m or Km as needed.
Response: We added this content in the revised manuscript, which is 8.5 km long for the first order stream and 6.9 km long for another order stream.

7) L156-160: Leachate/Water volumes used for the SPE? How did you avoid breakthrough?
Response: We actually realized this point. Before SPE, we estimated the maximum volume before loading samples based on the SPE recovery (60% in our case) and the final eluate concentration 40 μg C/ml. The exact loading volumes vary among samples, but the eluate concentration is similar that might help reduce the selective ionization. In the revised manuscript, we added detailed information on this issue. From line 160 to 166, we wrote as ‘They were solid-phase extracted (SPE) using the Bond Elut PPL

(Agilent Technologies, 100 mg PPL in 3 ml cartridge), following the procedures of Dittmar et al. (2008). In order to avoid overloading of the SPE column, the aliquot volume of SPE DOM was calculated based on an average SPE recovery (60% for permafrost DOM; Ward, et al., 2015) and a final eluate concentration of 40 μg C/ml (in ca. 2 ml methanol)." We also cited a reference 'Ward, C. P. and Cory, R. M.(2015) Chemical composition of dissolved organic matter draining permafrost soils. Geochimica Et Cosmochimica Acta. 167, 63-79.'.

8) L180: 'Freeze-dried retentates'? Meaning SPE-DOM? Explain or rephrase accordingly.
Response: We already changed into 'Freeze-dried retentates from ultrafiltration'.

9) L206-207: Does that mean the in-stream microbial generation of DOM is negligible?
Response: In this section we use optical properties to show DOM characteristics, in that way we could quick screen the inter-annual variation between year 2015 and 2016. The lack of inter-annual change did not mean insignificant microbial generation of DOM in stream. Actually, from headwater to downstream water, we observed apparent change in optical parameters of DOM, suggesting substantial transform of DOM by photo or bio-degradation. We discussed this point in section 3.3 Spatiotemporal change of 14C-DOC age through fluvial networks.

10) L213-216: I do not see any detailed discussion on this inter-annual variability. Please add.
Response: We added the discussion on inter-annual variability in the revised manuscript. From line 204-211 as 'Paired t-test based on S275-295 and SUVA254 of water samples showed no significant inter-annual variation between year 2015 and 2016 ($p = 0.716$ and $p = 0.321$, respectively). The mean S275-295 of 2015 and 2016 samples was (14.5 ± 0.48) × 10-3 nm-1 for the AL leachates and (18.3 ± 1.3) × 10-3 nm-1 for the PL leachates. In the stream waters, the S275-295 ranged from 15.8× 10-3 to 22.5 × 10-3 nm-1, increasing in downstream reaches."
In the stream waters, the $S_{275\text{-}295}$ ranged from 15.8×10^{-3} to 22.5×10^{-3} nm^{-1}, increasing in downstream reaches. Mean $SUVA_{254}$ was 3.52 ± 0.24 L mg C^{-1} m^{-1} for the AL leachates and 0.95 ± 0.14 L mg C^{-1} m^{-1} for the PL leachates, and decreased in the stream from Q-1 to Q-10 (3.06 to 1.27 L mg C^{-1} m^{-1}), and then remained low (Fig. 3). ', but for the radiocarbon age of the DOM, actually we did not do inter-annual analysis, here we discussed just temporally change in different months in 2015 as showed in line 219-221.

11) L243: Please expand on the discussion of these differences in chemical composition between AL and PL leachates. The information shown in the discussion is highly selective to age and very limited with regards to molecular composition and

optical properties. In the first paragraph on page 11 there is some discussion on this with regards to sample Q-1, but nothing much else (i.e. along the sampling transect).
Response: This is good comment. Actually, we have addressed this issue previously. Please see Wang, et al., 2018, Selective leaching of dissolved organic matter from alpine permafrost soils on the Qinghai-Tibetan Plateau. J. Geophys. Res. Biogeosci., 123, 1005-1016, doi: 10.1002/2017jg004343. In this article, we examined and compared the chemical composition of DOM leached from AL and PL. We found the selective leaching in Permafrost soils that upper AL leachates are enriched in aromatic components, whereas deep PL leachates are enriched in alkyl components. In current work, we focus on instream processes of DOM rather than leaching process from soil to headwater. Nevertheless, we added some sentences (line 249-252) as "This difference is likely attributed to selective release of aromatic components from upper AL soils and carbohydrate/protein components from deep PL soils during the thawing process which was observed in our previous study (Wang et al., 2018)." We also cite the reference of Want et al. (2018) in the revised manuscript.

12) L256: How were STDs obtained from n=2?
Response: We are sorry for this mistake. Here we calculated the average value and the average deviation based on two samples. In the revised manuscript, we corrected all the calculated data throughout the manuscript, and here rewrote as "The mean DOC concentration of the AL leachate based on samples from 2015 and 2016 (11.57 ± 0.77mg/L) is similar to that of the headstream (Q-1; ca. 11.69 ± 0.60 mg/L), but substantially lower than that of the PL leachates (126.40 ± 14.80 mg/L), supporting a predominance of AL-leachate DOM in stream waters. In addition, the $SUVA_{254}$ is 3.52 ± 0.17 L mg C^{-1} m^{-1} for AL leachates and 0.95 ± 0.10 L mg C^{-1} m^{-1} for PL leachates, whereas the $S_{275\text{-}295}$ is (14.49 ± 0.34) × 10^{-3} nm^{-1} for AL leachates and (18.05 ± 0.94) × 10^{-3} nm^{-1} for PL leachates".

13) L260: Remove the '(' before 'and'
Response: done.

14) L261-264: idem as above – explain differences in composition between AL and PL.
Response: We have added some brief information about AL and PL leachates at Line 267-269, but as mentioned above (response to comment 11), we did not give much detailed information in this study.

15) L280: What about seasonal variations in the optical properties and MS data? Missing important information here. Please add.
Response: It is a pity that we did not conduct FT-ICR MS analysis for seasonal samples. But a seasonal variation of DOM could be revealed by our optical analyses. In the revised manuscript, we added the sentence as 'Our result also shows seasonal

variations in 14C age and optical parameters of headstream DOM. From summer to fall, the SUVA254 of stream DOM at Q-1 decreased from 2.79 to 2.36 mg C-1 m-1, whereas the S275-295 increased from 16.33 × 10-3 to 16.96 × 10-3 nm-1. These temporal changes indicated that the proportion of aromatic components and high molecular weight compounds decreased with the deepening of permafrost thawing.' Please see the details from line 292 to 297.

16) L285-288: This statement seems to make sense, but at the same time the DOC concentration from PL is significantly more elevated compared to AL. How much is 'percolation' due to freezing reduced?
Response: We agree it would be helpful to distinguish leaching and percolate if we could separate them. Unfortunately, it is very difficult to monitor percolation in fieldwork. So we just separate the whole soil profile into active layer and permafrost layer and discussed combined effects by collecting leaching waters at the Q-1. Nevertheless, several lines of evidence from optical, DOC concentration and FT-ICRMS support our statement that active layer is a major contributor to leachate DOM.

17) Section 4.2: I encourage the authors to actually calculate physical dilution to see if it indeed agrees with the estimation determined based on age variation. Mineralization and in-stream contributions could be roughly estimated by difference based on dilution only.
Response: This is a good comment. We qualitatively discussed the dilution effect in line 305-312. Several lines of evidence from DOC concentration, total water discharge and water conductivity all supported the existence of dilution effect in downstream waters. However, it is difficult to quantify this effect because the lack of DOC and water flux data of tributaries and groundwater. We may conduct more comprehensive survey in next year and address this issue in future. In current study, we circumvent this problem by tracing unique peaks of DOM by using FT-ICRMS. If these unique peaks disappear along the stream, it suggests the occurrence of biodegradation or photodegradation for the specific type of compounds.

18) L304-314: Not clear why the authors make comparisons with values observed in coastal systems. Seems irrelevant in this case.
Response: We accepted this suggestion and removed related contents in the revised manuscript.

19) L314-318: The size-reactivity continuum (Amon and Benner, 1996) applies well for marine systems. However, it is controversial for terrestrial systems as both similar and opposite trends have been reported in the literature. Considering this, I would focus on the photo-degradation process, which is more likely dominant in this case.
Response: We agree with this suggestion and deleted these sentences. In line 343-344, we rewrote the sentence as 'A strong negative correlation between S275-295 and

SUVA254 ($R2 = 0.73$, $p < 0.01$) indicates that photodegradation of high molecular weight aromatic compounds (like lignin) may play a role in the decrease of mean molecular weight of DOM along the stream, despite that microbial degradation might also contribute the molecular modification in stream to less extent.'

20) L346-353: I would like to see an effort by the authors in enhancing the interpretation of the MS data here. Can molecular formulas generated/added along the transect through microbial in-stream activity be identified? What about photo-transformation products? I assume not all photo-degraded DOM is mineralized to CO2.

Response: Yes, besides the mineralized molecules and new produced molecules, the partial transformations of DOM can also contribute the change in molecular characteristics in stream. This kind of transformations is a result from combined factors such as microbial degradation, photo degradation, and also new input from base flow and instream generation, among others. In the revised manuscript, we have added a supporting figure (Fig. S1) that shows the change of DOM molecular formula between Q-1 and Q-17, with the decrease of aromatics and the addition of highly unsaturated molecules. From line 363 to 369, we rewrote the sentences as "Concurrent with the rapid loss of AL-specific formulas, some new molecular formulas were detected by FT-ICR MS, which was mainly attributed to in-situ production by stream algae/microbes, and import from groundwater and molecular transformation of leachate DOM. The van Krevelen diagram showed that the new products were mainly composed of highly unsaturated molecules (Fig. S1). The addition of new molecular formulas was also reflected by the 14C enrichment in middle and lower-stream (Fig. 3b)."

21) L392-393: This seems to make sense, but is still mainly speculative. Can you find partial evidence for this from your MS data (i.e. in-stream DOM)? Not sure it is possible.

Response: We identified some new formulas which give some evidence for in-stream production of new DOM, but as mentioned above, these new compounds could be also partially transformed from leachate DOM from bio-, and photo-degradation. In order to distinguish the different pathways, we are currently doing a series of incubation experiments in the laboratory, and wish we can publish those data soon..

22) L413: As above – seasonal variations discussion needs to be enhanced.

Response: We have added the discussion about seasonal changes in the revised manuscript. Please see our response to comment 15.

23) Figure 5: Color code 'dots' are VERY hard to see. Please enlarge accordingly.

Response: we have changed the figure legends and provide a new figure 5 in the revised

manuscript.

Interactive comment on "Spatiotemporal transformation of dissolved organic matter along an alpine stream flowpath on the Qinghai-Tibetan Plateau: importance of source and permafrost degradation" by Yinghui Wang et al.

Anonymous Referee #1
Received and published: 11 July 2018
We appreciate the anonymous reviewer to supply valuable comments, we accepted most of the comments. The follows are our point by point response, and the changes are marked in light blue in the revised manuscript.

General comments: The manuscript describes the use of multi techniques (UV, AMS, and FT-ICR MS) to characterize dissolved organic matter (DOM) and discuss the temporal and spatial transformation of DOM along an alpine stream. The methodologies are state-of-the-art, the study area will be of interest to readership, the discussion is appropriate, and the manuscript is well-written. There are some issues, listed below, to address prior to publication.

Specific comments:
Comment 1: Figure 5 was not mentioned in the context, which is my most concern. The "highly unsaturated compounds" was classified into L and H, how to define the classification?
Response: This is a good comment. In literatures on FT-ICRMS based chemical characterization for natural DOM, compounds are commonly divided into several groups according to elemental composition (e.g., C, H, O, N, S). In some case, the researchers further divided unsaturated compounds into high unsaturated and low unsaturated compounds according to a threshold value of O/C=0.5. In our manuscript, we actually did not distinguish the unsaturated low oxygen (O/C < 0.5) from the unsaturated high oxygen (O/C > 0.5). So we have grouped the 'U.H' and 'U.L' together and provides a new figure 5e in the revised manuscript.

Comment 2: From the distributions of H/C and O/C ratios shown in the van Krevelen diagrams in Figure 5, I trust the assignment of compounds is not credible. The authors directly used the data processing results from the software (EnviroOrg), however, the molecule assignment based on accurate mass value cannot guarantee a correct identification on the mass peak, especially on the high mass end.
Response: We somewhat agree with the reviewer. Assignment of molecular formulas in a complex mixture is challenging and this process would be nearly impossible, especially at relatively high m/z as the reviewer points out, if formulas were assigned to individual signals without context. However, in addition to exact mass, the compositional continuum of natural organic matter has been used for the past 15-20 years to assign molecular formulas to natural organic matter (Kujawinski ,E.B., 2002; Stenson, A., et al. 2003). The compositional patterns (homologous series) in natural organic matter enable us to assign molecular formulas to compounds associated with

high accurate signals at low m/z where there is only one possible formula. We then extrapolate formula assignment to those at high m/z (in combination with the use of accurate mass), as many researchers did. We added the references listed above to line 174 of the text, also at lines 513 and 568 as Kujawinski, E.B., (2002). Electrospray Ionization Fourier Transform Ion Cyclotron Resonance Mass Spectrometry (ESI FT-ICR MS): Characterization of Complex Environmental Mixtures. Environ. Forensics 3, 207-216., Stenson, A.C.; Marshall, A.G.; Cooper, W.T., (2003) Exact masses and chemical formulas of individual Suwannee River fulvic acids from ultrahigh resolution electrospray ionization Fourier transform ion cyclotron resonance mass spectra, Anal. Chem. 75, 1275-1284.

Comment 3: Most "compounds" classified into the CA area (O/C<0.2) should be incorrect assignment of mass peaks with high mass values. This does not mean the data processing and the discussion are wrong, in fact, most published papers in the past years have this problem.

Response: There have been some papers that show "islands" or isolate pockets (in van Krevelen space) of formulas that are classified as condensed aromatic compounds. In these cases, we agree with the reviewer that they might be misassigned formulas that are associated with signals of compounds at relatively high m/z. However, this is not the case here. In addition to using homologous series (see above) that is afforded to us by the compositional continuum of natural organic matter (NOM) to assign molecular formulas, we also ensure that the formulas assigned are continuous in carbon number molecular weight, aromaticity, and heteroatom content. The combination of these parameters along with homologous series and accurate mass provide several layers of verification for accurate formula assignments for complex mixtures. The van Krevelen diagrams in Figure 5 show that there are no discontinuities (islands) in the compositional continuum, an indicator (of several) that the formulas are assigned correctly.

Comment 4: In Table 1 and Table 2, as well as many places in the context, the number of assigned molecular formulas was used to discuss the composition of DOM and the degradation along the stream. This is not rigorous and could lead to misunderstanding for readers both on the mass spectrometry analysis and the environmental interpretation. Not like most other analysis instrument detectors, the limit of detection (LOD) of ESI FT-ICR MS for DOM analysis is uncertain, it partially determined by the most abundant peak in the spectrum. Briefly, less mass peaks do not means the composition of the sample is "simple" and compounds not detected in the sample does not means these compounds must in lower concentration. I suggest the authors provide some raw mass spectrometry data in the supporting information, such as the broad bound mass spectra, expanded mass scale mass spectra.

Response: We agree with the reviewer that interpreting environmental relevance based solely on changes in the number of assigned molecular formulas could be ambiguous. We also agree that changes in the number of assigned formulas is not

indicative of compounds at lower concentration as FT-ICR MS is better regarded as a qualitative rather than quantitative method. However, in our study, thousands of specific mass peaks were detected in headwater samples but not detected in downstream waters, providing an unambiguous evidence on compositional change of DOM along the stream. In addition, before the SPE process, we had done calculation to make sure each sample containing similar DOM concentrations for FT-ICR MS analysis. This step largely removed the difference in background matrix between samples. Given these fact, we are confident that the peaks lost in downstream are not only caused by the detection limit. In addition, optical and radiocarbon data also showed substantial changes along stream, supporting our assignment of FT-ICRMS data. Nevertheless, we have changed the term "molecular richness" to "chemodiversity" (as described by Kellerman et al. 2014) in lines 227 and 237 for clarity. Frankly speaking, we do not see any necessity of the addition of raw mass spectrum in supporting information. There are over ten thousand peaks in raw mass spectrum for leachate DOM, which reveal little useful information to readers without further data processes. As such, we decided not to do so. But we already provided the raw data in the excel in supporting information.

Line 220. The numbers include the isotope formulae?
Response: We did not include the isotopologues here.

Line 221. Elemental analysis was not mentioned in the context.
Response: We changed 'elemental' to 'molecular-level' for clarity.

Line 232. I don't think it is a good manner to compare the changes in MW and AI with percentage values.
Response: We removed the percentages from MW and AI.

Spatiotemporal transformation of dissolved organic matter along an alpine stream flowpath on the Qinghai-Tibetan Plateau: importance of source and permafrost degradation

Yinghui Wang [a,b], Robert G.M. Spencer [c], David C. Podgorski [d], Anne M. Kellerman [c], Harunur Rashid [a], Phoebe Zito [d], Wenjie Xiao [b], Dandan Wei [a], Yuanhe Yang [e], Yunping Xu [a*]

[a] *Shanghai Engineering Research Center of Hadal Science and Technology*, *College of Marine Sciences, Shanghai Ocean University, Shanghai 201306, China.*

[b] *Key Laboratory for Earth Surface Processes of the Ministry of Education, College of Urban and Environmental Sciences, Peking University, Beijing 100871, China.*

[c] *National High Magnetic Field Laboratory Geochemistry Group and Department of Earth, Ocean, and Atmospheric Science, Florida State University, Tallahassee, FL 32306, USA*

[d] *Pontchartrain Institute for Environmental Sciences, Department of Chemistry, University of New Orleans, New Orleans, LA, 70148, USA*

[e] *State Key Laboratory of Vegetation and Environmental Change, Institute of Botany, Chinese Academy of Sciences, Beijing 100093, China*

*Corresponding author. *E-mail*: ypxu@shou.edu.cn (Y. Xu)

Abstract The Qinghai-Tibetan Plateau (QTP) accounts for approximately 70% of global alpine permafrost and is an area sensitive to climate change. The thawing and mobilization of ice and organic carbon-rich permafrost impact hydrologic conditions and biogeochemical processes on the QTP. Despite numerous studies of Arctic permafrost, there are no reports to date for the molecular-level in-stream processing of permafrost-derived dissolved organic matter (DOM) on the QTP. In this study, we examine temporal and spatial changes of chemical composition of DOM and ^{14}C age of dissolved organic carbon (DOC) along an alpine stream (3850–3207 m above sea level) by Fourier transform ion cyclotron resonance mass spectrometry (FT-ICR MS), accelerator mass spectrometry (AMS) and UV-visible spectroscopy. Compared to downstream sites, the DOM at the headstream exhibited older radiocarbon (^{14}C-DOC) age, higher mean molecular weight, higher aromaticity and fewer polyunsaturated components. At the molecular level, 6409 and 1345 formulas were identified as unique to the active layer (AL) leachate and permafrost layer (PL) leachate, respectively. Comparing permafrost leachates to the downstream site, 59% of AL-specific formulas and 90% of PL-specific formulas were degraded, likely a result of rapid instream degradation of permafrost-derived DOM. From peak discharge in the summer to low flow in late autumn, the DOC concentration at the headstream site decreased from 13.9 to 10.2 mg/L, while the ^{14}C-DOC age increased from 745 to 1560 years before present (BP), reflecting an increase in relative contribution of deep permafrost carbon due to the effect of changing hydrological conditions over the course of the summer on DOM source (AL vs. PL). Our study thus demonstrates that hydrological conditions impact the mobilization of permafrost carbon in an alpine fluvial network, the signature of which is quickly lost through instream mineralization and transformation.

Keywords: dissolved organic matter; permafrost; Qinghai-Tibet Plateau; FT-ICR MS;

radiocarbon age

1. INTRODUCTION

The amount of carbon stored in permafrost is roughly twice as much as that in the atmosphere and represents the largest component of the terrestrial carbon pool (Zimov et al., 2006; Tarnocai et al., 2009). Accelerated climate warming has led to a succession of changes associated with permafrost thaw, where liquid water once frozen in permafrost soils has changed watershed hydrology, topography and ecosystem biogeochemistry (Frey and Smith, 2005; Abbott et al., 2015; Vonk et al., 2015). When permafrost-derived carbon enters aquatic system, it can be rapidly mineralized and transformed by microbes and light (Cory et al., 2014; Drake et al., 2015; Vonk et al., 2015). Therefore, the mobilization of carbon from permafrost soils where it has been relatively stable for thousands of years into dissolved carbon could increase greenhouse gas emissions (Cory et al., 2013; Vonk et al., 2013; Mann et al., 2015; Ward and Cory, 2016; Selvam et al., 2017) and exacerbate climate warming via a positive feedback loop (Koven et al., 2011; Schuur et al., 2015).

The seasonal thawing-freezing cycle of permafrost soils could change hydrologic condition and restrict source water contributions to river flow, leading to variability in the flux and the chemical composition of dissolved organic matter (DOM) in permafrost-impacted watersheds (Petrone et al., 2006; Laudon et al., 2011). DOM in the Yukon River exhibits seasonal changes in aromaticity, molecular weight, ^{14}C age and biodegradability (Striegl et al., 2007; Spencer et al., 2008; Wickland et al., 2012; O'Donnell et al., 2014). Since the persistence of DOM in aquatic systems is related to chemical composition (Kellerman et al., 2015; Kellerman et al., 2018), substituting space for time to trace changes in DOM composition along a hydrologic flowpath may

illustrate the environmental behavior and fate of seasonally exported permafrost carbon.

The Qinghai-Tibet Plateau (QTP), the world's largest and highest plateau, plays a critical role in the evolution of the Asian Monsoon (Sato and Kimura, 2007; Wu et al., 2007) and supplies water to several large rivers such as the Yangtze River, Yellow River and Yarlung Tsangpo (Yao et al., 2007; Kang et al., 2010). As a climate sensitive region, the QTP has experienced significant warming since the 1950s (Qiu, 2008) with the mean annual air temperature rising at a rate of 0.36 °C per decade from 1961 to 2007 (Wang et al., 2008). Consequently, the permafrost soils on the QTP have begun to thaw and collapse, causing abundant carbon loss from degradation, leaching and lateral displacement (Mu et al., 2016). However, compared with an abundance of studies on Arctic permafrost, biogeochemical studies on QTP permafrost are scant (Mu et al., 2016). This results in a limited understanding of the permafrost carbon cycle as a whole since the QTP represents nearly 10% of the global permafrost, what's more, the QTP differs from the Arctic in altitude, climate, and hydrology (Bockheim and Munroe, 2014).

Here, we conducted a study on the spatial and temporal change of permafrost-derived DOM on the northeastern QTP. We applied multiple analytical techniques including Fourier transform ion cyclotron resonance mass spectrometry (FT-ICR MS), AMS radiocarbon (^{14}C), and UV-visible optical spectroscopy. Our objective is two-fold: 1) determine the dominant sources of alpine stream DOM on the QTP (active layer (AL) vs. permafrost layer (PL)), and 2) trace the persistence and degradation of permafrost-derived DOM in an alpine fluvial network. This work represents the first step in characterizing in-stream removal and transformation processes of permafrost carbon at the molecular level on the QTP.

2. MATERIALS AND METHODS

2.1. Study area and sampling

Our study area is located in Gangcha County, north of Qinghai Lake. The climate is typical plateau continental climate, characterized by extensive sunshine duration (~3000 hours per year), long cold and dry winters and short cool and humid summers (Peng et al., 2015). During 2013-2016, January had the lowest average monthly temperature (–11.82 °C), while December had the lowest average monthly precipitation (0.3 mm). Meanwhile, the highest average monthly temperature and precipitation occurred in July (11.66 °C) and August (124.67 mm), respectively. These climate data are available at http://data.cma.cn. The permafrost soil was developed in the late Quaternary, and accumulated > 2 m thick in mountainous areas of the Gangcha County. Due to the rapid climate warming on the QTP, the ice-rich permafrost began to thaw, and several thermo-erosion gullies formed a decade ago. In this study, we focused on a continuous system that starts with a thermo-erosion gully (> 200 m long), forms a stream which flows into Qinghai Lake, the largest lake in China with a surface area of ca. 4500 km^2. Thawed permafrost slumping exposed soil profiles at the gullies' head (ca. 3850 meters above sea level; masl). The top 60 cm is an active layer (AL) that comprises abundant grass litter and roots, underlain by a dark permafrost layer (PL) without visible plant debris. The thaw depth reached 78 cm in August 2015. Seasonal thaw of the entire AL and the upper PL allows for both vertical and lateral percolation of rainwater, which mobilizes large amounts of particulate and dissolved organic matter. The water in the gully flows southward across the hillslope before draining into Qinghai Lake, and the total length of the stream is around 40 km (Fig. 1).

Our fieldwork was conducted in the summer and autumn of 2015 and 2016. In 2015, a time-series sampling campaign was conducted at the headstream (Q-1) from August

120 1st when the warm and humid climate caused the largest export of leachates, to October
121 15th when the leaching ceased due to little precipitation and low temperature. On August
122 1st of 2016 and 2017, AL and PL leachates were collected at the depth of 60 cm and 220
123 cm, respectively, of the gullies' head. 20 L HDPE carboys were cleaned by pure water,
124 0.1 N hydrochloric acid and pure water prior to use. It usually took 2 days to gather >
125 15 L leaching waters. After that, the leachate samples were immediately kept on ice and
126 in the dark by aluminum foil. They were transported to the temporary laboratory in the
127 Gangcha County within 6 hours. Besides soil leachates, water samples (20 L each) were
128 collected from twenty sites along the stream (Fig. 1). Sampling sites Q-1 to Q-10 are
129 located in a first-order stream (ca. 8.5 km long) that originates in the largest thermo-
130 erosion gully, whereas sites Q-11 and Q-12 are located in another first-order stream
131 nearby (ca. 6.9 km long). These two streams merge together to form the main stream,
132 along which sampling sites Q-13 to Q-20 were located. Surface water samples were
133 collected using pre-cleaned HDPE carboys and kept on ice and in the dark until filtering
134 through Whatman GF/F filters (0.7 μm) within 6 hours after sampling. To obtain enough
135 carbon for ^{14}C analyses, aliquots of the 0.7 μm filtrate were concentrated over a cross-
136 flow ultrafiltration system with 1 kDa cut off (Millipore®, Pellicon 2 system). The
137 retentates and the remaining filtrate were all stored at –20 ºC until further analysis. All
138 glassware and GF/F filters were combusted at 450 ºC for at least 4 hours prior to use.
139
140 **2.2. Hydrological condition, DOC concentration and spectral absorbance in alpine**
141 **streams**
142 On Aug. 1st 2015, stream water temperature, pH and conductivity were measured
143 with a portable Horiba W-23XD Water Quality Monitoring System. The water flux was
144 calculated according to flow rate and cross-sectional area of the stream. The DOC

concentration of each water sample was determined by 3-5 injections on a Shimadzu TOC-V_{CPH} analyzer using high temperature combustion, and the coefficient of variance across measurements was < 2%.

The optical properties of the water samples were determined using a Shimadzu UV-1800 spectrophotometer. The scan range was between 200 and 800 nm and Milli-Q water (18.2 MΩ cm^{-1}) was used as the blank. A quartz cell with 1.0 cm path length was used. The spectral slope of the 275–295 nm region ($S_{275\text{-}295}$), an indicator for the molecular weight of DOM (Helms et al., 2008), was determined by applying log linear fits across the wavelengths 275–295 nm. Specific UV absorbance ($SUVA_{254}$), an indicator for relative aromatic C content, was calculated by dividing the decadic UV absorbance at 254 nm with DOC concentration (Weishaar et al., 2003).

2.3. Electrospray ionization Fourier transform ion cyclotron resonance mass spectrometry (ESI FT-ICR MS)

Selected water samples collected in 2016 from headstream (Q-1), mid-stream (Q-9), and downstream (Q-17), as well as leachate samples collected from the AL and PL, were prepared for FT-ICR MS analyses. They were solid-phase extracted (SPE) using the Bond Elut PPL (Agilent Technologies, 100 mg PPL in 3 ml cartridge), following the procedures of Dittmar et al. (2008). In order to avoid overloading of the SPE column, the aliquot volume of SPE DOM was calculated based on an average SPE recovery (60% for permafrost DOM; Ward et al., 2015) and a final eluate concentration of 40 µg C/ml (in 2 ml methanol). The methanol extracts were analyzed on a 9.4 Tesla custom-built FT-ICR MS at the National High Magnetic Field Laboratory (NHMFL; Tallahassee, FL; Kaiser et al., 2011). The injection speed was 0.7 µL/min. A total of 100 broadband scans was accumulated for each mass spectra. Other instrumental parameters can be found in

Hodgkins et al. (2016). After internal calibration in MIDAS Predator Analysis (NHMFL), formulas were assigned based on published rules to peaks with intensities > 6σ baseline noise (Stubbins et al., 2010) using EnviroOrg®™ software and categorized by compound class based on the elemental composition of molecular formulas (Kujawinski, 2002; Stenson et al. 2003; Spencer et al., 2014; Corilo, 2015). A modified aromaticity index (AI_{mod}) was calculated according to the definition of Koch and Dittmar (2006): $AI_{mod} = \frac{1+C-0.5O-S-0.5(H+N+P)}{C-0.5O-S-N}$, and if AI_{mod} is negative, then AI=0. The groups referenced in this study are: 1) aliphatics (Ali.): H/C 1.5 - 2.0, O/C < 0.9, N = 0; 2) peptides (Pep.): H/C 1.5 - 2.0, O/C < 0.9, N > 0; 3) highly unsaturated compounds (Uns.): AI_{mod} < 0.5, H/C < 1.5; 4) polyphenols (Pol.): 0.5 < AI_{mod} < 0.67; 5) condensed aromatics (CA): $AI_{mod} \geq 0.67$. The relative abundance of the defined compound class was weighted by signal magnitude in each spectrum.

2.4. Radiocarbon analyses

Freeze-dried retentates from ultrafiltration were fumigated with concentrated hydrochloric acid (12 M) in order to remove inorganic carbon. After that, the samples were analyzed on the Keck Carbon Cycle Accelerator Mass Spectrometry (AMS) Facility at the University of California, Irvine, USA. Processing blank and sample preparation backgrounds were subtracted. Radiocarbon concentrations are given as conventional ^{14}C age following Stuiver and Reimer (1993).

3. RESULTS

3.1. Hydrology and DOC concentration from headstream to downstream water

Discharge increased along the stream reach, from 0.15 m^3/min at the headstream (Q-1) on August 1st 2015 to 24.14 m^3 /min (Q-19) (Fig. 2). pH increased from 7.4 at Q-

1 to 8.2 at Q-4 and remained elevated in the middle and lower stream (7.9 to 8.4). Conductivity was relatively constant from Q-1 to Q-6 (35 to 38 μs/cm), then increased at Q-7 and remained elevated downstream (48 to 60 μs/cm). The DOC concentration was high in headstream waters (e.g., 11.69 ± 0.60 mg/L at Q-1 and 10.22 ± 1.09 mg/L at Q-2; Mean ± AD, same hereafter) and decreased downstream (3.29 ± 0.75 to 4.73 ± 0.21 mg/L from Q-5 to Q-20). The mean DOC concentration of the AL leachates (11.57 ± 0.77 mg/L) was an order of magnitude lower than that of the PL leachates (126.40 ± 14.80 mg/L).

3.2. Optical properties of DOM in leachates and stream waters

Paired t-test based on $S_{275\text{-}295}$ and $SUVA_{254}$ of water samples showed no significant inter-annual variation between year 2015 and 2016 ($p = 0.716$ and $p = 0.321$, respectively). The mean $S_{275\text{-}295}$ of 2015 and 2016 samples was $(14.49 \pm 0.34) \times 10^{-3}$ nm^{-1} for the AL leachates and $(18.05 \pm 0.94) \times 10^{-3}$ nm^{-1} for the PL leachates. In the stream waters, the $S_{275\text{-}295}$ ranged from 16.05×10^{-3} to 21.80×10^{-3} nm^{-1}, increasing in downstream reaches. The mean $SUVA_{254}$ was 3.53 ± 0.17L mg C^{-1} m^{-1} for the AL leachates and 0.95 ± 0.10L mg C^{-1} m^{-1} for the PL leachates, and decreased in the stream from Q-1 to Q-11 (2.92 to 1.66 L mg C^{-1} m^{-1}), and then remained low (Fig. 3). A strong negative correlation was found between $SUVA_{254}$ and $S_{275\text{-}295}$ for water samples from both years ($R^2 = 0.77$, $P < 0.01$).

3.3. Spatiotemporal change of ^{14}C-DOC age through fluvial networks

^{14}C-DOC age of the PL leachate was 4145 years BP, which was much older than that of the AL leachate (535 years BP; Fig. 4a). The ^{14}C-DOC age decreased along the stream from 745 years BP for the headstream water (Q-1) to 160 years BP at Q-19, a

site close to Qinghai Lake. Besides apparent spatial variability, the ^{14}C-DOC age also changed temporally. In 2015, the ^{14}C-DOC age of the headstream water (Q-1) increased from 745 years BP on August 1st, to 1015 years BP on August 11th and 1560 years BP on September 5th (Fig. 4b).

3.4. FT-ICR MS characterization of SPE-DOM

Compared with the PL leachate, the AL leachate was characterized by higher molecular chemodiversity (14709 vs. 9645 assigned formulae), higher mean molecular weight (498.81 vs. 452.73 Da) and higher AI_{mod} (0.47 vs. 0.30). Molecular-level composition revealed that compounds containing both N and S were only detected in the AL leachates and headstream waters. The AL leachate contained 54.28% highly unsaturated compounds, 27.10% polyphenols and 17.23% condensed aromatic compounds, whereas the proportion of aliphatics and peptides was minor (ca. 1.30%). Compared with the AL leachate, the PL leachate comprised a higher proportion of polyunsaturated compounds (74.23%) and aliphatics + peptides (10.04%), but a lower proportion of polyphenols (11.33%) and condensed aromatics (4.32%).

Along the stream (Q-1, Q-9, and Q-17), the molecular chemodiversity, mean molecular weight and modified aromaticity index of SPE-DOM decreased from 14924 to 11074, 510.1 to 486.5 Da and 0.43 to 0.36, respectively (Table 1). The relative abundance of aromatics (condensed aromatics and polyphenols) decreased by 48% (35.7% at Q-1 vs. 18.4% at Q-17), whereas that of highly unsaturated compounds increased by 28% (62.8% at Q-1 vs. 80.3% at Q-17). Aliphatics and peptides were minor components of stream DOM (<1.3%) and did not exhibit a downstream trend.

4. DISSCUSSION

4.1. AL leachates as a major source of stream DOM

The UV-visible optical parameters and molecular formulas resolved by FT-ICR MS show that the AL and PL leachates have different chemical compositions (Table 1 and 2). This difference is likely attributed to selective release of aromatic components from AL and carbohydrate/protein components from deep PL during the soil thawing process which was observed in our previous study (Wang et al., 2018). Since chemical composition impacts the reactivity of DOM (Kellerman et al., 2015), the differing chemical composition between the AL and PL leachates that enter the stream may influence bioavailability (Vonk et al., 2013) and photolability (Stubbins et al., 2017). Thus, distinguishing DOM source is crucial for understanding in-stream biogeochemical processes in permafrost-impacted systems. DOM may originate from a variety of sources including permafrost soil (AL and PL) leaching, in-situ microbial production, and wet deposition from snow and rain. At the headstream site (Q-1), however, the dominant source of DOM is permafrost soil leaching, as short residence times at the gully head restrict in-stream production and wet deposition is likely negligible due to low DOC concentrations in Tibetan glaciers (0.2-3.3 μg/ml; Spencer et al., 2014). Assuming that headstream DOM is derived only from permafrost soil leaching, we are able to estimate the relative contributions of DOM from the AL and PL.

The mean DOC concentration of the AL leachate based on samples from 2015 and 2016 (11.57 ± 0.77 mg/L) is similar to that of the headstream (Q-1; ca. 11.69 ± 0.60 mg/L), but substantially lower than that of the PL leachates (126.40 ± 14.80 mg/L), supporting a predominance of AL-leachate DOM in stream waters. In addition, the $SUVA_{254}$ is 3.52 ± 0.17 L mg C^{-1} m^{-1} for AL leachates and 0.95 ± 0.10 L mg C^{-1} m^{-1} for PL leachates, whereas the $S_{275\text{-}295}$ is (14.49 ± 0.34) × 10^{-3} nm^{-1} for AL leachates and

(18.05 ± 0.94) × 10^{-3} nm^{-1} for PL leachates. Similar optical properties and DOC concentrations between AL-leachates and the headstream water (3.52 ± 0.17 L mg C^{-1} m^{-1} vs 2.92 ± 0.13 L mg C^{-1} m^{-1} for $SUVA_{254}$ and (14.49 ± 0.34) × 10^{-3} nm^{-1} vs (16.05 ± 0.28) × 10^{-3} nm^{-1} for $S_{275\text{-}295}$) support DOM that leaches from the AL dominates stream DOM. Furthermore, the stream water at Q-1 has a ^{14}C-DOC age of 745 years BP, close to that of the AL leachate (535 years BP), and much younger than that of the PL leachate (4145 years BP). We estimate the portion of AL and PL-derived C by using a binary mixing model based on $\Delta^{14}C$ values of bulk DOC (Criss, 1999):

$$\Delta^{14}C_{DOM} = f_{AL} \times \Delta^{14}C_{AL} + f_{PL} \times \Delta^{14}C_{PL}$$

$$1.0 = f_{AL} + f_{PL}$$

According to this model, ca. 94% of DOC collected from stream site Q-1 on Aug. 1, 2015 originated from the AL (Fig. 6a). Headstream ^{14}C-DOC age increased from summer to fall (Fig. 4b), reflecting an enhanced contribution of old carbon from the deeper soils (i.e., PL), however, the AL still accounted for ≥ 72% of total DOC exported (Fig. 6a). This binary mixing model may overestimate the contribution of AL to stream DOC since PL-derived DOC may be degraded faster than AL-derived DOC, due to the high biolability of ancient permafrost carbon as shown in Arctic ecosystems (Vonk et al., 2013). Nonetheless, the AL appears as a major contributor to stream DOC in the QTP.

Seasonal variation of ^{14}C-DOC (Fig. 4b) has been previously observed in high latitude permafrost areas in Alaska (Aiken et al., 2014; O'Donnell et al., 2014), with the most enriched ^{14}C values observed in the spring and becoming more depleted through summer-fall and/or during winter. Our result also shows seasonal variations in ^{14}C age and optical parameters of headstream DOM. From summer to fall, the $SUVA_{254}$ of stream DOM at Q-1 decreased from 2.79 to 2.36 mg C^{-1} m^{-1}, whereas the $S_{275\text{-}295}$

295 increased from 16.33 × 10^{-3} to 16.96 × 10^{-3} nm^{-1}. These temporal changes indicated that
296 the proportion of aromatic components and high molecular weight compounds
297 decreased with the deepening of permafrost thawing. The mean monthly air temperature
298 of Gangcha County, after reaching the maximum in July (ca. 10.5 ºC), decreases to 2.1
299 ºC in September (data from http://data.cma.cn). As air temperature drops, surface soils
300 freeze earlier than deeper soils, leading to an increase in the relative contribution of
301 deep soil carbon (i.e. PL) to stream DOM, although the DOC concentration in Q-1
302 decreased from 13.87 mg/L to 10.22 mg/L (Fig. 6b).
303
304 **4.2. Selective removal of DOM along the alpine stream on the QTP**
305 The DOC concentration decreased (11.69 to 3.29 mg/L) from upper to mid-stream
306 (Q-1 to Q-5), which could be attributed to a dilution effect and/or in-stream degradation
307 of DOM. Dilution from groundwater is likely since groundwater discharge sustains
308 baseflow of rivers and streams in the QTP (Ge et al., 2008). Downstream groundwater
309 inputs were further supported by the order of magnitude increase in discharge (1.49 to
310 24.14 m^3/min) and increase in conductivity (37 to 60 μs/cm). Moreover, downstream
311 DOC concentrations remained about 3.0-4.0 mg/L (Q-15 to Q-20), indicative of the low
312 DOC concentrations of groundwater. Conversely, a tributary that originated from
313 another thermo-erosion gully merged into the study stream, however, the different
314 tributaries exhibited similar DOC concentrations (e.g., Q-9 and Q-10 vs. Q-11 and Q-
315 12; Fig. 2d). The similarities in DOC concentrations were attributed to homogeneity in
316 dominant vegetation, soil type and climate, and thus, homogeneity in DOM inputs to
317 the different tributaries in our study area. Therefore, additional tributaries could not
318 explain the spatial pattern of DOC concentration.
319 Despite evident dilution, DOC attenuation could be partly due to in-stream

degradation given several lines of evidence from optical properties, radiocarbon age and molecular composition. The UV-visible optical parameters, $S_{275\text{-}295}$ and $SUVA_{254}$, have been widely used to reveal mean molecular weight and aromaticity of DOM, respectively (Weishaar et al., 2003; Helms et al., 2008; Spencer et al., 2009; Mann et al., 2012). ~~In our study, the $S_{275\text{-}295}$ of stream waters varied from 15.8 × 10^{-3} to 22.5 × 10^{-3} nm^{-1} (Fig. 3a), comparable to typical riverine DOM values (13.19 × 10^{-3} to 22.96 × 10^{-3} nm^{-1}), but much lower than that of DOM from continental shelf and slope (29.7 × 10^{-3} to 48.5 × 10^{-3} nm^{-1}) (Fichot and Benner, 2012), suggesting a moderate degradation of stream DOM on the QTP.~~ A downstream increase for $S_{275\text{-}295}$ regardless of sampling time (Fig. 3a) reflects selected degradation of high molecular weight compounds, leading to the enrichment of low molecular weight DOM. ~~This spatial trend is in accordance with the size-reactivity continuum model (Amon and Benner, 1996) that the bioreactivity of DOM decreases along a continuum of size (from large to small).~~ In addition to $S_{275\text{-}295}$, $SUVA_{254}$ varied from 1.50 to 2.92 L mg C^{-1} m^{-1}, showing a general decrease downstream (Fig. 3b). Lignin, an aromatic biopolymer specific for vascular plants (Hedges et al., 1997), is relatively resistant to biodegradation (Hedges et al., 1985), but highly photo-labile (Lanzalunga and Bietti, 2000). Cory et al. (2014) found that sunlight accounts for 70% to 95% of water column carbon processing in Arctic rivers and lakes. Given strong solar radiation and long sunshine duration (~3000 hours per year) on the QTP (Peng et al., 2015), photo-degradation could be an important pathway for carbon removal in QTP streams. A strong negative correlation between $S_{275\text{-}295}$ and $SUVA_{254}$ (R^2 = 0.73, p < 0.01) indicates that photodegradation of high molecular weight aromatic compounds (like lignin) may play a role in the decrease of mean molecular weight of DOM along the stream, despite that microbial degradation might also contribute the molecular modification in stream.

345 Similar to $SUVA_{254}$ and $S_{275-295}$, the data from FT-ICR MS also show a downstream
346 decrease in aromaticity (AI_{mod}: 0.43 to 0.36) and mean molecular weight of stream
347 DOM (510.0 to 486.5 Da; Table 1). Compared with headstream DOM at Q-1, DOM at
348 Q-9 and Q-17 was characterized by a lower proportion of condensed aromatics and
349 polyphenols and enriched in highly unsaturated compounds (Table 1). The decrease in
350 relative abundance of aromatic compounds is consistent with the reports for the
351 photolability of aromatic formulas within permafrost, river and ocean DOM (Stubbins
352 and Dittmar, 2015; Stubbins et al., 2017).
353 As discussed in section 4.1, AL is the principal contributor to stream DOM. Thus,
354 tracing AL-derived DOM is paramount in estimating biogeochemical processes of
355 carbon in the stream. FT-ICR MS identified 6409 molecular formulas specific to AL-
356 leachates (i.e. not observed in the PL, Table 2). Through various stream processes, some
357 AL specific formulas were removed from the DOM pool (from 17% by Q-1 up to 59%
358 by Q-17), which accounted for 66% of the aromatic compounds and 51% of the highly
359 unsaturated compounds (Table 2). Molecular formulas containing N and/or S were more
360 labile in the fluvial networks than CHO formulas, with 84% of S-containing formulas
361 and 100% of S and N-containing formulas lost (Table 2). Furthermore, the removal of
362 DOM formulas (ca. 83% of AL-specific formulas, and >95% of AL-specific formulas)
363 occurred in upper and mid-stream (leachates to Q-9). Concurrent with the rapid loss of
364 AL-specific formulas, some new molecular formulas were detected by FT-ICR MS,
365 which was mainly attributed to in-situ production by stream algae/microbes, an import
366 from groundwater and molecular transformation of leachate DOM. The van Krevelen
367 diagram showed that the new products were mainly composed of highly unsaturated
368 molecules (Fig. S1). The addition of new molecular formulas was also reflected by the
369 ^{14}C enrichment in middle and lower-stream (Fig. 3b).

370 Overall, our multiple analyses demonstrate a rapid and selective degradation of
371 stream DOM on the QTP. The attenuation of aromatic compounds and enrichment of
372 highly unsaturated compounds could change the environmental photo- and bio-lability
373 of DOM, increasing relative importance of photodegradation in upper stream and
374 biodegradation in lower stream. The continuous change in chemical properties of DOM
375 along the alpine stream flowpath has a potential to shift the aquatic microbial
376 community since DOM serves as an important energy and nutrient source(Wild et al.,
377 2014).
378
379 **4.3. Prediction of in stream carbon dynamic under continued warming**
380 The DOC concentrations, UV-visible optical parameters and FT-ICR MS all suggest
381 that currently, PL is a minor source to stream DOM (see 4.1). However, the QTP is a
382 sensitive area to global warming, with a rate of air temperature rise that is
383 approximately three times the global warming rate (Qiu, 2008). According to climate
384 model predictions, spatial average temperatures of the QTP will increase by 0.68–0.98
385 ^{o}C for the period of 2015–2050 (Zhu et al., 2013), and in 2050, the mean AL thickness
386 on the QTP permafrost will increase by approximately 0.3-0.8 m more than that in 2010
387 (Zhang and Wu, 2012). With the deepening of the AL, carbon that is currently stable in
388 the PL will be thawed and mobilized into the downslope aquatic environments, which
389 inevitably changes the proportion of AL vs. PL contributions to stream DOM. Thus, it
390 is worth to trace chemical change of PL leachates along the stream. The PL leachate
391 contained only 1345 formulas unique to the PL leachate in comparison to the AL,
392 accounting for 14% of total assigned formulas (Table 2). Most PL-specific formulas
393 were more biolabile components, e.g. aliphatics and peptides (73%), followed by highly
394 unsaturated formulas (23.6%) and aromatics (1.9%). At the downstream site (i.e., Q-

17), 90% of these PL-specific molecular formulas were lost, substantially higher than that of AL-specific formulas (59%). Furthermore, the vast majority of PL-specific formulas were lost within < 1 km (Q-1: 83%) whereas only 17% of AL-specific formulas were lost by Q-1 (Table 2). Therefore, the FT-ICR MS data demonstrate that permafrost thaw can trigger a rapid degradation of old carbon that was frozen in soils for thousands of years (Fig. 3a). This is consistent with findings in Arctic fluvial networks that show the utilization of ancient permafrost carbon in headstream waters was rapid (Mann et al., 2015; Frey et al., 2016). Therefore, we hypothesize that with enhanced leaching of deep soil C under continued warming on the QTP, DOM in alpine streams will be more enriched in biolabile aliphatics/peptides and depleted in photolabile aromatics

Finally, despite substantial in-stream degradation, some old permafrost-derived carbon (i.e., polyphenols and highly unsaturated compounds) could persist downstream. In addition, CO_2 produced by respiration of old DOC could be utilized by stream algae to biosynthesize new DOM with an old carbon age. These effects resulted in a sustained deviation from modern ^{14}C-DOC age in the alpine stream (e.g., 160 years BP at Q-19), and were even detected in large rivers on the QTP (e.g., Yangtze River and Yellow River; Qu et al., 2017). Thus, under continued warming, a greater quantity of older C may be transported into large watersheds on the QTP, and thereby exert an important role in biogeochemical cycles there since older carbon has different photo and bio-lability from young carbon in AL soils.

5. CONCLUSIONS

Permafrost thaw represents positive feedbacks to climate change, but its carbon alteration and removal mechanism is not well known, particularly for the alpine

permafrost such as the QTP. Here we use multiple analytical methods (e.g., FT-ICR MS, radiocarbon and UV-visible spectroscopy) to trace spatial and temporal variability of permafrost DOM along an alpine stream in the northeastern QTP, from which four conclusions have been reached.

1) Presently, the AL is the major source to stream DOM with relatively high aromaticity. This character, combined with strong solar radiation on the QTP, suggests sunlight may be an important driver for DOM removal in alpine fluvial networks, which was corroborated by an almost 60% loss of AL specific formulas from the thermo-erosion gully head to downstream waters.

2) From summer to fall (seasonal permafrost thawing to freezing cycle), the concentrations and chemical composition of stream DOM varied significantly at the thermo-erosion gully head. Even though the total amount of the leached DOC decreased, the contribution of deep permafrost carbon with lower aromaticity and lower MW increased, reflected by an increase of ^{14}C-DOC age and a decrease in aromaticity of DOM.

3) Although both the AL and PL leachate DOM underwent rapid degradation in the alpine stream, some components with old ^{14}C-DOC age (mainly highly unsaturated) were recalcitrant to degradation and could be transported downstream, causing ^{14}C-DOC values that were more depleted than modern radiocarbon age downstream in our study, and even in large watersheds as observed in Qu et al. (2017).

4) With deepening of the AL under continued climate warming on the QTP, currently stable PL soils will thaw and release greater amounts of old, aliphatic/peptide-rich DOM to downstream waters. This change in source and chemical composition will make microbial degradation more important for carbon removal and may shift downstream microbial communities, even in large watershed systems. All these factors

should be taken into account when interpreting alpine permafrost carbon dynamics under the amplified climate warming trend on the QTP.

ACKNOWLEDGEMENTS

This work was financially supported by the National Basic Research Program of China (2014CB954001). Y.W. thanks the China Scholarship Council for supporting study in the United States of America as a joint Ph. D. student. We thank Futing Liu, Yanyan Yan, Shangzhe Zhou, Xinyu Zhang for assistance in the field. FT-ICR MS was supported by NSF (DMR-1157490).

References

Abbott, B.W., Jones, J.B., Godsey, S.E., Larouche, J.R. and Bowden, W.B. (2015) Patterns and persistence of hydrologic carbon and nutrient export from collapsing upland permafrost. Biogeosciences 12, 3725-3740.

Aiken, G.R., Spencer, R.G.M., Striegl, R.G., Schuster, P.F. and Raymond, P.A. (2014) Influences of glacier melt and permafrost thaw on the age of dissolved organic carbon in the Yukon River basin. Global Biogeochem. Cycles 28, 525-537.

Bockheim, J.G. and Munroe, J.S. (2014) Organic Carbon Pools and Genesis of Alpine Soils with Permafrost: A Review. Arct. Antarct. Alp. Res. 46, 987-1006.

Corilo, Y.E. (2015) EnviroOrg. Florida State University.

Cory, R.M., Crump, B.C., Dobkowski, J.A. and Kling, G.W. (2013) Surface exposure to sunlight stimulates CO_2 release from permafrost soil carbon in the Arctic. Proc. Natl. Acad. Sci. USA 110, 3429-3434.

Cory, R.M., Ward, C.P., Crump, B.C. and Kling, G.W. (2014) Sunlight controls water

column processing of carbon in arctic fresh waters. Science 345, 925-928.

Criss, R.E. (1999) Principles of stable isotope distribution. Oxford University Press, New York.

Dittmar, T., Koch, B., Hertkorn, N. and Kattner, G. (2008) A simple and efficient method for the solid-phase extraction of dissolved organic matter (SPE-DOM) from seawater. Limnol. Oceanogr. Methods 6, 230-235.

Drake, T.W., Wickland, K.P., Spencer, R.G., McKnight, D.M. and Striegl, R.G. (2015) Ancient low-molecular-weight organic acids in permafrost fuel rapid carbon dioxide production upon thaw. Proc. Natl. Acad. Sci. USA 112, 13946-13951.

Frey, K.E. and Smith, L.C. (2005) Amplified carbon release from vast West Siberian peatlands by 2100. Geophys. Res. Lett. 32, doi: 10.1029/2004GL022025.

Frey, K.E., Sobczak, W.V., Mann, P.J. and Holmes, R.M. (2016) Optical properties and bioavailability of dissolved organic matter along a flow-path continuum from soil pore waters to the Kolyma River mainstem, East Siberia. Biogeosciences 13, 2279-2290.

Ge, S., Wu, Q.B., Lu, N., Jiang, G.L. and Ball, L. (2008) Groundwater in the Tibet Plateau, western China. Geophys. Res. Lett. 35, 80-86.

Hedges, J.I., Cowie, G.L., Ertel, J.R., James Barbour, R. and Hatcher, P.G. (1985) Degradation of carbohydrates and lignins in buried woods. Geochim. Cosmochim. Acta 49, 701-711.

Hedges, J.I., Keil, R.G. and Benner, R. (1997) What happens to terrestrial organic matter in the ocean? Org. Geochem. 27, 195-212.

Helms, J.R., Stubbins, A., Ritchie, J.D., Minor, E.C., Kieber, D.J. and Mopper, K. (2008) Absorption spectral slopes and slope ratios as indicators of molecular weight, source, and photobleaching of chromophoric dissolved organic matter. Limnol. Oceanogr. 53, 955-969.

Hodgkins, S.B., Tfaily, M.M., Podgorski, D.C., Mccalley, C.K., Saleska, S.R., Crill, P.M., Rich, V.I., Chanton, J.P. and Cooper, W.T. (2016) Elemental composition and optical properties reveal changes in dissolved organic matter along a permafrost thaw chronosequence in a subarctic peatland. Geochim. Cosmochim. Acta 187, 123-140.

Kaiser, N.K., Quinn, J.P., Blakney, G.T., Hendrickson, C.L. and Marshall, A.G. (2011) A novel 9.4 tesla FTICR mass spectrometer with improved sensitivity, mass resolution, and mass range. J. Am. Soc. Mass Spectrom. 22, 1343-1351.

Kang, S., Xu, Y., You, Q., Flügel, W.-A., Pepin, N. and Yao, T. (2010) Review of climate and cryospheric change in the Tibetan Plateau. Environ. Res. Lett. 5, doi:10.1088/1748-9326/1085/1081/015101.

Kellerman, A.M., Guillemette, F., Podgorski, D.C., Aiken, G.R., Butler, K.D. and Spencer, R.G.M. (2018) Unifying Concepts Linking Dissolved Organic Matter Composition to Persistence in Aquatic Ecosystems. Environ. Sci. Technol., doi: 10.1021/acs.est.1027b05513.

Kellerman, A.M., Kothawala, D.N., Dittmar, T. and Tranvik, L.J. (2015) Persistence of dissolved organic matter in lakes related to its molecular characteristics. Nat. Geosci. 8, 454-457.

Koch, B.P. and Dittmar, T. (2006) From mass to structure: an aromaticity index for high-resolution mass data of natural organic matter. Rapid Commun. Mass Spectrom. 20, 926-932.

Koven, C.D., Ringeval, B., Friedlingstein, P., Ciais, P., Cadule, P., Khvorostyanov, D., Krinner, G. and Tarnocai, C. (2011) Permafrost carbon-climate feedbacks accelerate global warming. Proc. Natl. Acad. Sci. U. S. A. 108, 14769-14774.

Kujawinski, E.B., (2002). Electrospray ionization fourier transform ion cyclotron resonance mass spectrometry (ESI FT-ICR MS): Characterization of complex

environmental mixtures. Environ. Forensics 3, 207-216.

Lanzalunga, O. and Bietti, M. (2000) Photo- and radiation chemical induced degradation of lignin model compounds. J. Photochem. Photobiol. B: Biol. 56, 85-108.

Laudon, H., Berggren, M., Ågren, A., Buffam, I., Bishop, K., Grabs, T., Jansson, M. and Köhler, S. (2011) Patterns and dynamics of dissolved organic carbon (DOC) in boreal streams: the role of processes, connectivity, and scaling. Ecosystems 14, 880-893.

Mann, P.J., Davydova, A., Zimov, N., Spencer, R.G.M., Davydov, S., Bulygina, E., Zimov, S. and Holmes, R.M. (2012) Controls on the composition and lability of dissolved organic matter in Siberia's Kolyma River basin. J. Geophys. Res. Biogeosci. 117, doi:10.1029/2011jg001798.

Mann, P.J., Eglinton, T.I., McIntyre, C.P., Zimov, N., Davydova, A., Vonk, J.E., Holmes, R.M. and Spencer, R.G. (2015) Utilization of ancient permafrost carbon in headwaters of Arctic fluvial networks. Nat. Commun. 6, doi:10.1038/ncomms8856.

Mu, C., Zhang, T., Zhang, X., Li, L., Guo, H., Zhao, Q., Cao, L., Wu, Q. and Cheng, G. (2016) Carbon loss and chemical changes from permafrost collapse in the northern Tibetan Plateau. J. Geophys. Res. Biogeosci. 121, doi:10.1002/2015JG003235.

O'Donnell, J.A., Aiken, G.R., Walvoord, M.A., Raymond, P.A., Butler, K.D., Dornblaser, M.M. and Heckman, K. (2014) Using dissolved organicmatter age and composition to detect permafrost thaw in boreal watersheds of interior Alaska. J. Geophys. Res. Biogeosci. 119, 2155-2170.

Peng, S., Du, Q., Wang, L., Lin, A. and Hu, B. (2015) Long-term variations of ultraviolet radiation in Tibetan Plateau from observation and estimation. Int. J. Climatol. 35, 1245-1253.

Petrone, K.C., Jones, J.B., Hinzman, L.D. and Boone, R.D. (2006) Seasonal export of

545 carbon, nitrogen, and major solutes from Alaskan catchments with discontinuous
546 permafrost. J. Geophys. Res. Biogeosci. 111, doi:10.1029/2006JG000281.
547 Qiu, J. (2008) The third pole. Nature 454, 393-396.
548 Qu, B., Sillanpää, M., Li, C., Kang, S., Stubbins, A., Yan, F., Aho, K.S., Zhou, F. and
549 Raymond, P.A. (2017) Aged dissolved organic carbon exported from rivers of the
550 Tibetan Plateau. PLoS One 12, e0178166, doi:
551 0178110.0171371/journal.pone.0178166.
552 Sato, T. and Kimura, F. (2007) How does the Tibetan Plateau affect the transition of
553 Indian monsoon rainfall? Mon. Weather Rev. 135, 2006-2015.
554 Schuur, E.A.G., McGuire, A.D., Schadel, C., Grosse, G., Harden, J.W., Hayes, D.J.,
555 Hugelius, G., Koven, C.D., Kuhry, P., Lawrence, D.M., Natali, S.M., Olefeldt, D.,
556 Romanovsky, V.E., Schaefer, K., Turetsky, M.R., Treat, C.C. and Vonk, J.E. (2015)
557 Climate change and the permafrost carbon feedback. Nature 520, 171-179.
558 Selvam, B.P., Lapierre, J.-F., Guillemette, F., Voigt, C., Lamprecht, R.E., Biasi, C.,
559 Christensen, T.R., Martikainen, P.J. and Berggren, M. (2017) Degradation potentials of
560 dissolved organic carbon (DOC) from thawed permafrost peat. Sci. Rep. 7,
561 doi:10.1038/srep45811.
562 Spencer, R.G., Aiken, G.R., Wickland, K.P., Striegl, R.G. and Hernes, P.J. (2008)
563 Seasonal and spatial variability in dissolved organic matter quantity and composition
564 from the Yukon River basin, Alaska. Global Biogeochem. Cycles 22, doi:
565 10.1029/2008GB003231.
566 Spencer, R.G.M., Aiken, G.R., Butler, K.D., Dornblaser, M.M., Striegl, R.G. and
567 Hernes, P.J. (2009) Utilizing chromophoric dissolved organic matter measurements to
568 derive export and reactivity of dissolved organic carbon exported to the Arctic Ocean:
569 a case study of the Yukon River, Alaska. Geophys. Res. Lett. 36, 141-153.

570 Spencer, R.G.M., Guo, W., Raymond, P.A., Dittmar, T., Hood, E., Fellman, J. and
571 Stubbins, A. (2014) Source and biolability of ancient dissolved organic matter in glacier
572 and lake ecosystems on the Tibetan Plateau. Geochim. Cosmochim. Acta 142, 64-74.
573 Stenson, A.C.; Marshall, A.G.; Cooper, W.T., (2003) Exact masses and chemical
574 formulas of individual Suwannee River fulvic acids from ultrahigh resolution
575 electrospray ionization Fourier transform ion cyclotron resonance mass spectra, Anal.
576 Chem. 75, 1275-1284.
577 Striegl, R.G., Dornblaser, M.M., Aiken, G.R., Wickland, K.P. and Raymond, P.A. (2007)
578 Carbon export and cycling by the Yukon, Tanana, and Porcupine rivers, Alaska, 2001–
579 2005. Water Resour. Res. 43, doi:10.1029/2006WR005201.
580 Stubbins, A. and Dittmar, T. (2015) Illuminating the deep: Molecular signatures of
581 photochemical alteration of dissolved organic matter from North Atlantic Deep Water.
582 Mar. Chem. 177, 318-324.
583 Stubbins, A., Mann, P.J., Powers, L., Bittar, T.B., Dittmar, T., McIntyre, C.P., Eglinton,
584 T.I., Zimov, N. and Spencer, R.G.M. (2017) Low photolability of yedoma permafrost
585 dissolved organic carbon. J. Geophys. Res. Biogeosci. 122, 200-211.
586 Stubbins, A., Spencer, R.G.M., Chen, H.M., Hatcher, P.G., Mopper, K., Hernes, P.J.,
587 Mwamba, V.L., Mangangu, A.M., Wabakanghanzi, J.N. and Six, J. (2010) Illuminated
588 darkness: Molecular signatures of Congo River dissolved organic matter and its
589 photochemical alteration as revealed by ultrahigh precision mass spectrometry. Limnol.
590 Oceanogr. 55, 1467-1477.
591 Stuiver, M. and Reimer, P.J. (1993) Extended ^{14}C Data Base and Revised Calib 3. 0 14C
592 Age Calibration Program. Radiocarbon 35, 215-230.
593 Tarnocai, C., Canadell, J.G., Schuur, E.A.G., Kuhry, P., Mazhitova, G. and Zimov, S.
594 (2009) Soil organic carbon pools in the northern circumpolar permafrost region. Global

595 Biogeochem. Cycles 23, doi:10.1029/2008gb003327.
596 Vonk, J.E., Mann, P.J., Davydov, S., Davydova, A., Spencer, R.G.M., Schade, J.,
597 Sobczak, W.V., Zimov, N., Zimov, S., Bulygina, E., Eglinton, T.I. and Holmes, R.M.
598 (2013) High biolability of ancient permafrost carbon upon thaw. Geophys. Res. Lett.
599 40, 2689-2693.
600 Vonk, J.E., Tank, S.E., Bowden, W.B., Laurion, I., Vincent, W.F., Alekseychik, P.,
601 Amyot, M., Billet, M.F., Canario, J., Cory, R.M., Deshpande, B.N., Helbig, M., Jammet,
602 M., Karlsson, J., Larouche, J., MacMillan, G., Rautio, M., Anthony, K.M.W. and
603 Wickland, K.P. (2015) Reviews and syntheses: Effects of permafrost thaw on Arctic
604 aquatic ecosystems. Biogeosciences 12, 7129-7167.
605 Wang, B., Bao, Q., Hoskins, B., Wu, G. and Liu, Y. (2008) Tibetan Plateau warming
606 and precipitation changes in East Asia. Geophys. Res. Lett. 35, 63-72.
607 Wang, Y., Xu, Y., Spencer, R.G.M., Zito, P., Kellerman, A., Podgorski, D., Xiao, W.,
608 Wei, D., Rashid, H. and Yang, Y. (2018) Selective leaching of dissolved organic matter
609 from alpine permafrost soils on the Qinghai-Tibetan Plateau. J. Geophys. Res.
610 Biogeosci., 123, 1005-1016.
611 Ward, C. P. and Cory, R. M.(2015) Chemical composition of dissolved organic matter
612 draining permafrost soils. Geochim. Cosmochim. Acta 167, 63-79.
613 Ward, C.P. and Cory, R.M. (2016) Complete and Partial Photo-oxidation of Dissolved
614 Organic Matter Draining Permafrost Soils. Environ. Sci. Technol. 50, 3545-3553.
615 Weishaar, J.L., Aiken, G.R., Bergamaschi, B.A., Fram, M.S., Fujii, R. and Mopper, K.
616 (2003) Evaluation of specific ultraviolet absorbance as an indicator of the chemical
617 composition and reactivity of dissolved organic carbon. Environ. Sci. Technol. 37,
618 4702-4708.
619 Wickland, K.P., Aiken, G.R., Butler, K., Dornblaser, M.M., Spencer, R.G.M. and Striegl,

620 R.G. (2012) Biodegradability of dissolved organic carbon in the Yukon River and its
621 tributaries: Seasonality and importance of inorganic nitrogen. Global Biogeochem.
622 Cycles 26, doi:10.1029/2012GB004342.
623 Wild, B., Schnecker, J., Alves, R.J.E., Barsukov, P., Bárta, J., Čapek, P., Gentsch, N.,
624 Gittel, A., Guggenberger, G., Lashchinskiy, N., Mikutta, R., Rusalimova, O.,
625 Šantrůčková, H., Shibistova, O., Urich, T., Watzka, M., Zrazhevskaya, G. and Richter,
626 A. (2014) Input of easily available organic C and N stimulates microbial decomposition
627 of soil organic matter in arctic permafrost soil. Soil Biol. Biochem. 75, 143-151.
628 Wu, G., Liu, Y., Zhang, Q., Duan, A., Wang, T., Wan, R., Liu, X., Li, W., Wang, Z. and
629 Liang, X. (2007) The influence of mechanical and thermal forcing by the Tibetan
630 Plateau on Asian climate. J. Hydrometeorol. 8, 770-789.
631 Yao, T., Pu, J., Lu, A., Wang, Y. and Yu, W. (2007) Recent glacial retreat and its impact
632 on hydrological processes on the Tibetan Plateau, China, and surrounding regions. Arct.
633 Antarct. Alp. Res. 39, 642-650.
634 Zhang, Z.Q. and Wu, Q.-B. (2012) Predicting changes of active layer thickness on the
635 Qinghai-Tibet Plateau as climate warming. J. Glaciol. Geocryol. 34, 505-511.
636 Zhu, X., Wang, W. and Fraedrich, K. (2013) Future climate in the Tibetan Plateau from
637 a statistical regional climate model. J. Clim. 26, 10125-10138.
638 Zimov, S.A., Schuur, E.A.G. and Chapin, F.S. (2006) Permafrost and the global carbon
639 budget. Science 312, 1612-1613.
640
641

Figure and table captions

Fig. 1. Location of the QTP and sampling sites Q1 to Q20. Sites marked by a star were selected for FT-ICR MS and ^{14}C-DOC analyses. The AL and PL denote the sampling locations of the active and permafrost layers. The blue line and the red line represent the first order and second order stream, respectively, and the blue dashed line denotes stream without GPS data.

Fig. 2. (a) Stream water discharge, (b) pH, and (c) conductivity at the sampling sites in 2015; and (d) DOC concentration in stream water and PL/AL leachates collected in 2015 (filled circles) and 2016 (open circles).

Fig. 3. UV-visible optical indices of the stream water and PL/AL leachate samples collected in 2015 (filled circles) and 2016 (open circles) on the QTP: $S_{275\text{-}295}$ (a) and $SUVA_{254}$ (b).

Fig. 4. Variations of ^{14}C-DOC age across the alpine stream spatially (a), and at headstream Q-1 temporally (b).

Fig. 5. van Krevelen diagrams of AL leachate DOM (a), PL leachate DOM (b), headstream DOM Q-1 (c), downstream DOM Q-17 (d), the relative abundance of defined compound class in different samples (e). CA = condensed aromatics, Pol. = polyphenols, Uns. = highly unsaturated compounds, Ali. = aliphatics, Pep. = peptides; and Sug. = Sugar.

Fig. 6. (a) Relative contribution of AL leachate DOM to headstream DOM (Q-1); and (b) temporal variation of the DOC concentration at headstream Q-1.

Table 1 The number of molecular formulas assigned, modified aromaticity index (AI_{mod}), mean molecular weight (mean MW) and relative abundance of defined compound classes detected by FT-ICR MS for DOM samples from the QTP, including soil leachates (AL and PL) and stream waters (Q-1, Q-9 and Q-17). CA = condensed aromatics, Pol. = polyphenols, Uns. = highly unsaturated compounds, Ali. = aliphatic, Pep. = peptides.

Table 2 The number of specific molecules identified in the AL leachate DOM and the PL leachate DOM within the fluvial network, and the percentage of peaks totally degraded during the transportation.

Supplementary Figure S1. Van Krevelen diagrams showing the molecular changes of DOM from head to down-stream on the QTP. The blue and red dots denote decreasing trends and increasing trends, respectively. The color gradient shows the percentage of change. The lines separating compound categories [a]aliphatics and peptides [b] highly unsaturated compounds [c] polyphenols [d] condensed aromatics based on rules in the methods are just for visualization, and the exact categorization may differ.

680 Fig. 1

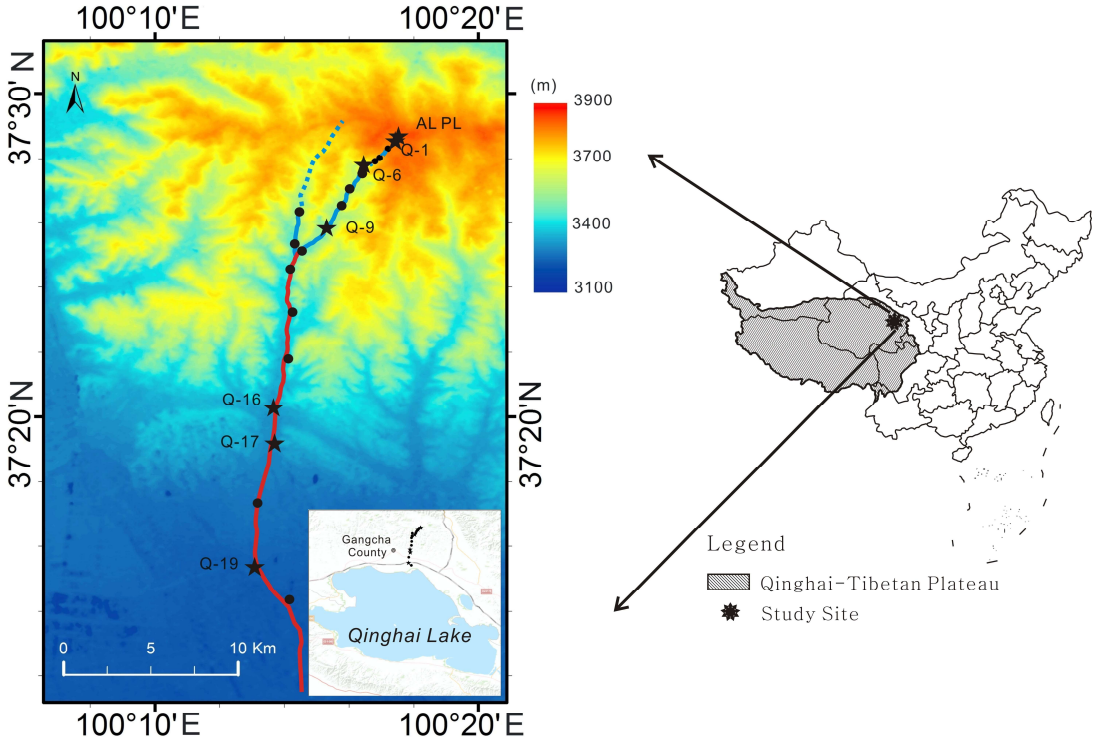

681

682

683 Fig. 2

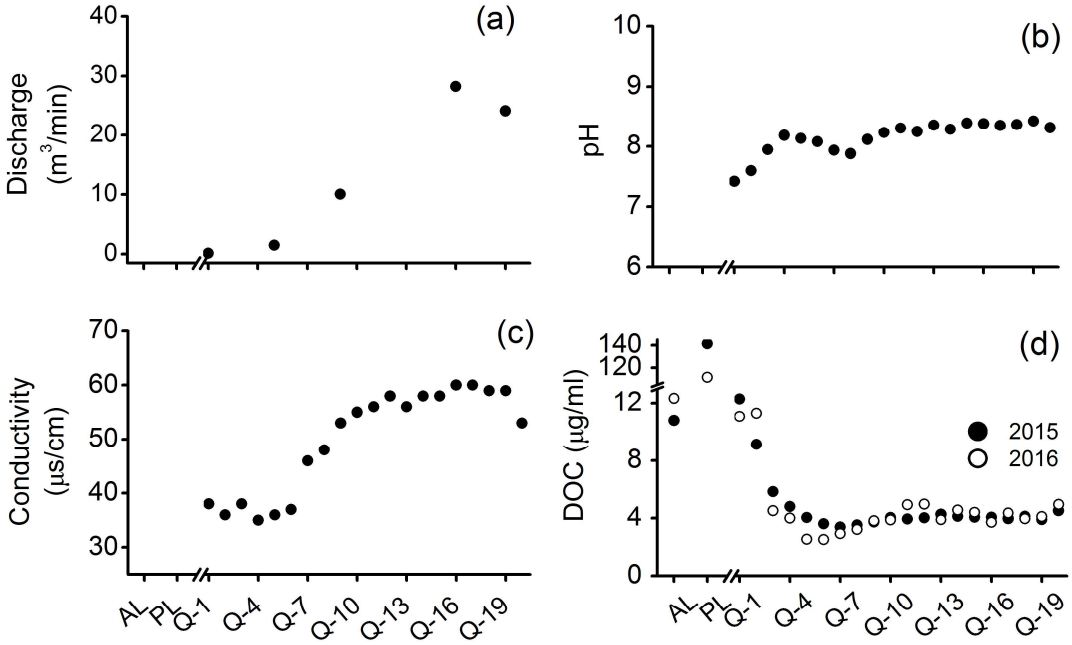

684

685

686 Fig. 3

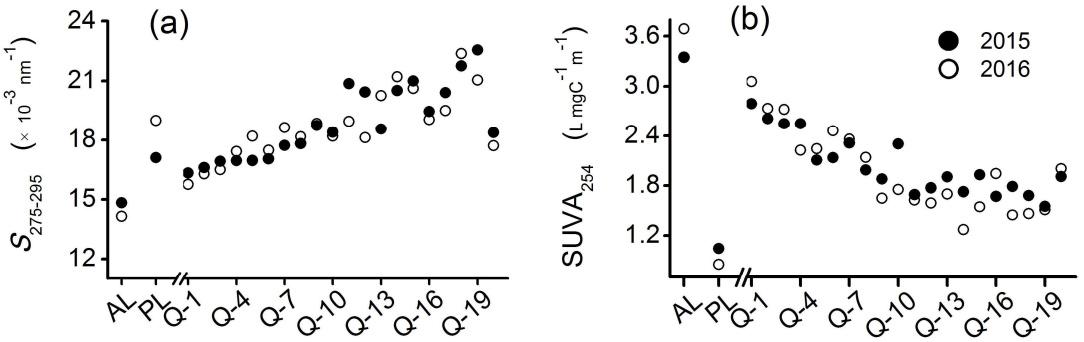

687

688

689 Fig. 4

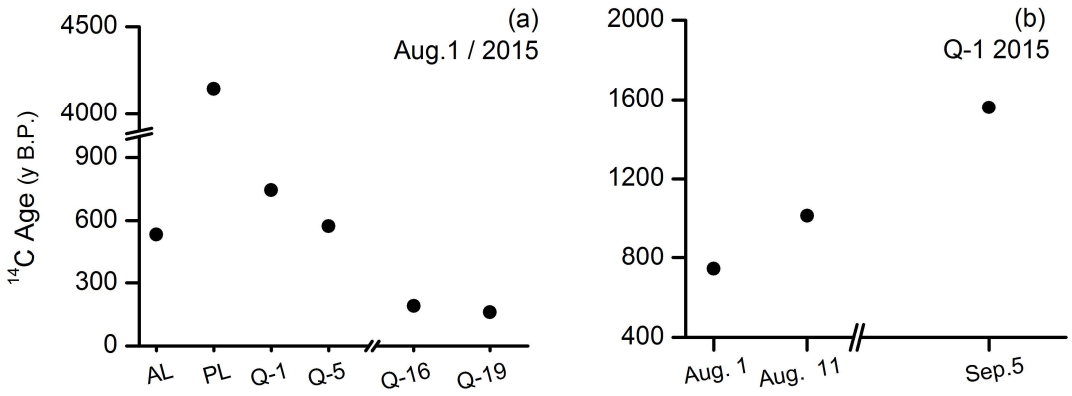

690

691

692 Fig. 5

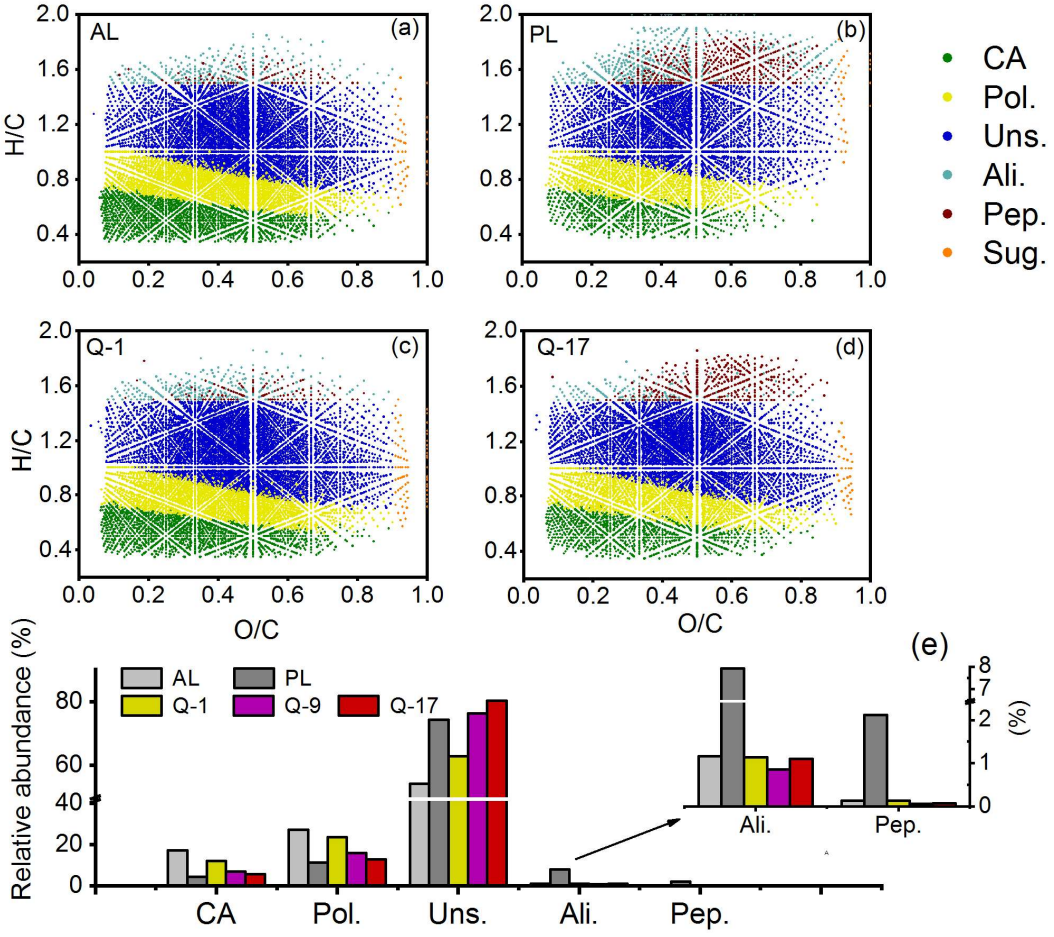

693

694

695 Fig. 6

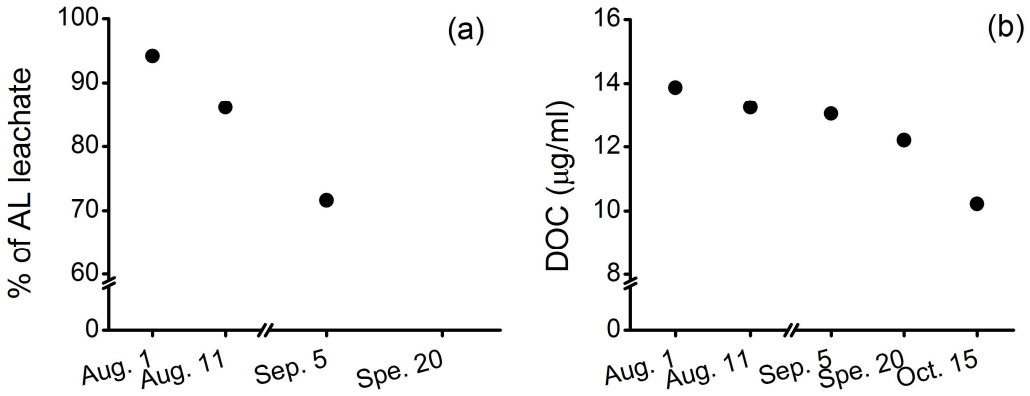

696

697

Table 1. The number of molecular formulas assigned, modified aromaticity index (AI_{mod}), mean molecular weight (mean MW) and relative abundance of defined compound classes detected by FT-ICR MS for DOM samples from the QTP, including soil leachates (AL and PL) and stream waters (Q-1, Q-9 and Q-17). CA = condensed aromatics, Pol. = polyphenols, Uns. = highly unsaturated compounds, Ali. = aliphatic, Pep. = peptides.

Sample	Formulas assigned	Mean MW	AI_{mod}	CA (%)	Pol. (%)	Uns. (%)	Ali. (%)	Pep. (%)
AL	14709	498.81	0.47	17.23	27.10	54.28	1.16	0.14
PL	9645	452.73	0.30	4.32	11.33	74.23	7.92	2.12
Q-1	14924	510.07	0.43	12.05	23.69	62.85	1.14	0.14
Q-9	11724	500.19	0.38	6.86	15.82	76.32	0.86	0.06
Q-17	11074	486.50	0.36	5.53	12.91	80.31	1.11	0.08

Table 2: The number of specific molecules identified in the AL leachate DOM and the PL leachate DOM within the fluvial network, and the percentage of peaks totally degraded during the transportation.

Samples		All peaks	Only CHO	Contains N	Contains S	Contains N& S	Condensed aromatics	Polyhoenols	Unsatuated	Aliphatics	Peptides
AL specific	AL	6409	1793	3370	424	822	1620	1720	2970	38	23
	Q-1	5311 (17%)	1653 (8%)	2791 (17%)	349 (18%)	517 (37%)	1278 (21%)	1416 (18%)	2549 (14%)	20 (47%)	14 (39%)
	Q-9	3365 (47%)	1294 (28%)	1917 (43%)	153 (64%)	0 (100%)	748 (54%)	838 (51%)	1759 (41%)	6 (84%)	1 (96%)
	Q-17	2623 (59%)	985 (45%)	1570 (53%)	67 (84%)	0 (100%)	550 (66%)	602 (65%)	1453 (51%)	5 (87%)	0 (100%)
PL specific	PL	1345	515	551	278	0	2	23	318	597	385
	Q-1	222 (83%)	90 (83%)	102 (81%)	30 (89%)	0	0 (100%)	11 (52%)	126 (60%)	46 (92%)	36 (91%)
	Q-9	117 (91%)	44 (91%)	46 (92%)	27 (90%)	0	2 (0%)	14 (39%)	96 (70%)	1 (100%)	4 (99%)
	Q-17	130 (90%)	47 (91%)	55 (90%)	28 (90%)	0	2 (0%)	13 (43%)	104 (67%)	6 (99%)	5 (99%)

Figure S1.

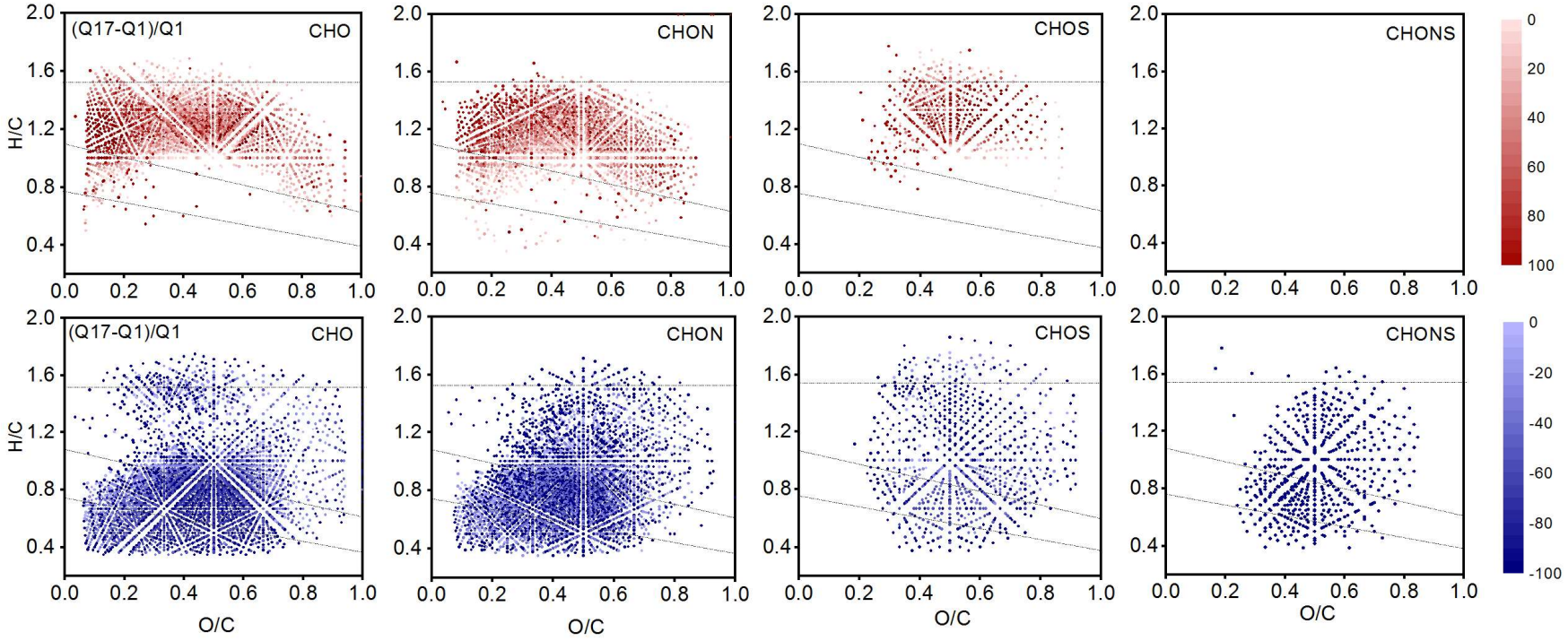
(Q17-Q1)/Q1
CHO
CHON
CHOS
CHONS
H/C
O/C
0
20
40
60
80
100
-20
-40
-60
-80
-100